

Original Article

TREX1 suppression imparts cancer-stem-cell-like characteristics to CD133⁻ osteosarcoma cells through the activation of E2F4 signaling

Jinyi Feng^{1,2*}, Ruilong Lan^{2*}, Guanxiong Cai², Jianhua Lin³

¹Department of Orthopedics, The First Affiliated Hospital of Xiamen University, Xiamen, China; Departments of ²Central Laboratory, ³Orthopaedics, The First Affiliated Hospital of Fujian Medical University, Fuzhou, Fujian, China. *Equal contributors.

Received December 5, 2018; Accepted January 22, 2019; Epub April 1, 2019; Published April 15, 2019

Abstract: There is ongoing debate whether cancer stem cells (CSCs) could arise from the transformation of non-CSCs under specific conditions. In the present study, the role of the three prime repair exonuclease 1 (TREX1) in regulating CSC generation from human osteosarcoma cells was investigated. High, intermediate and low levels of TREX1 expression were respectively observed in low-grade, high-grade and metastatic human osteosarcoma samples, while the opposite tendency was observed for E2F4, a transcription factor associated with G2 arrest. Luciferase assay proved that TREX1 had a negative impact on the activity of *E2F4* promoter. TREX1 was highly expressed in CD133⁻ HOS cells (non-CSC osteosarcoma cells) compared to CD133⁺ ones; whereas TREX1 knockdown endowed the CD133⁻ non-CSCs with CSC-like characteristics *in vitro* relying on E2F4 activation, as demonstrated by enlarged proportion of the subset expressing CSC markers in flow cytometry analysis, enhanced self-renewal ability in osteosphere formation assay, increased metastasis capacity in migration and invasion assays, together with improved chemoresistance to cisplatin. Furthermore, TREX1 knockdown and subsequent E2F4 activation could promote the tumorigenicity of CD133⁻ non-CSCs *in vivo*. With respect to underlying mechanisms, it was found that in CD133⁻ HOS cells, TREX1 suppression would allow the activation of β -catenin signaling in the dependence of E2F4, thus possibly leading to the up-regulation of the transcription factor OCT4. These findings suggested that TREX1 was probably a negative regulator of CSC formation and hence worth to be further studied for developing new treatments in cancer therapies targeting CSCs.

Keywords: TREX1, cancer stem cells (CSCs), E2F4, β -catenin signaling, OCT4, osteosarcoma

Introduction

Accumulating evidence over the last years confirmed the existence of a cell population that may comprise 0.1% to 20% of the tumor tissue and is capable of promoting tumor initiation, self-propagation, and differentiation; these cells were so-called cancer stem cells (CSCs) [1]. The membrane-bound pentaspan glycoprotein CD133 was frequently expressed on CSCs and regarded as one of the classic CSC markers in various carcinomas [2, 3]. Additional cell surface markers had also been identified, such as CD117 and Stro-1 [4, 5]. CD117 and Stro-1 double positive cells possessed the major characteristics of CSCs, including higher metastatic potential, increased chemoresistance, retention of multipotent differentiation ability and

considerable reconstitution capacity upon serial transplantation [4, 5]. OCT4, Nanog, Sox-2 and KLF4 are known transcription factors playing significant roles in tumor cell fate, regulating cell proliferation, cell survival, and the tumor-initiating properties of CSC-like cells [6, 7].

There is dispute over the origin of CSCs. It remains unclear whether CSCs are derived from a mature tissue stem cell that has undergone malignant change or has developed from a terminally-differentiated cell that de-differentiates to re-initiate a stemness program, following malignant transformation [8-12]. Osteosarcomas are the most common non-hematologic malignant tumors of bone in childhood and adolescence [13]. Compelling evidence indicates that osteosarcoma contains CSCs [14-16]. A

thorough understanding of the origin as well as the characteristic signaling of CSCs are required for the development of targeted therapies for osteosarcoma.

Three prime repair exonuclease 1 (TREX1) is the major 3' DNA exonuclease in mammalian cells. Mutations in the human *TREX1* gene have been linked to autoimmune diseases [17]. The dominant *TREX1* mutations associated with the autoimmune diseases result in defective exonuclease activity during double-stranded DNA (dsDNA) degradation [18]. Also, the association of TREX1 expression with the incidence of various kinds of cancer has been characterized by previous studies. For example, a significant difference in cytoplasmic and nuclear expression of TREX1 between cancer and paracancerous tissues ($P=0.038$ and <0.001 , respectively) of esophageal squamous cell carcinoma has been reported [19]. TREX1 has been implicated as a putative methylation specific biomarker in neuroblastoma [20], whereas single nucleotide polymorphisms of TREX1 have been shown to be associated with overall survival of pancreatic cancer patients [21]. However, the functions and regulatory mechanisms of TREX1 in tumors are still relatively poorly characterized. In particular, very little is known regarding the expression of TREX1 in osteosarcoma, and more importantly, its roles in the initiation and progression of osteosarcoma with respect to regulation of CSC generation.

Our recent study on clinical samples has revealed that the level of TREX1 may be negatively related to metastasis in patients with osteosarcoma, and point out preliminarily the lower expression of TREX1 in CD133⁺ subset of osteosarcoma cell lines when compared to CD133⁻ subset [22]. In the present study, a more detailed analysis concerning the expression and clinical relevance of TREX1 was carried out in human osteosarcoma samples with a larger size; furthermore, the role of TREX1 in the regulation of CSC generation, and the signaling involved in these processes were explored.

Materials and methods

Clinical specimen and data collection

The use of tissue samples and patient information was approved by the Ethics Committee of

the First Affiliated Hospital, Fujian Medical University. Written informed consents were taken from all the participants, and ethical guidelines under Declaration of Helsinki were followed.

Specimens from 94 cases of primary untreated osteosarcoma (non-metastatic: low-grade [n=9] and high-grade [n=34]; metastatic [n=51]) were collected between January 2004 and January 2013 in the Department of Pathology, First Affiliated Hospital, Fujian Medical University, Fuzhou, Fujian, China. Total cellular RNA of human osteosarcoma samples was extracted for quantitative real-time PCR. The formalin-fixed and paraffin-embedded surgical tumor samples were performed with immunohistochemical (IHC) staining. Following the review of the medical records and the contact of the patients and/or their relatives by telephone, the required follow-up information was obtained until December 31, 2014. The relevant clinical data recorded in the present study included gender, age, tumor location, tumor size, local recurrence status, lung metastasis status and overall survival.

Immunohistochemical (IHC) staining

For IHC analysis, tissue samples were stained with anti-TREX1 (1:200) or anti-E2F4 (1:100) antibodies (Abcam, Carlsbad, CA, USA), and each sample was evaluated [23]. The percentage of TREX1 and/or E2F4-positive tumor cells was counted and categorized according to four levels: <2%, 2%-10%, 11%-50%, and 51%-100%.

Cell culture

Human osteosarcoma cell lines HOS, MG63, SW1353 and U2OS were obtained from the American Type Culture Collection (ATCC, Manassas, VA, USA), and maintained in Dulbecco's modified Eagle's medium (DMEM; Sigma-Aldrich, St Louis, MO, USA) supplemented with 10% fetal bovine serum (FBS; Atlanta Biologicals, Lawrenceville, GA, USA), 100 U/ml penicillin and 100 µg/ml streptomycin (Invitrogen, Carlsbad, CA, USA).

FACS cell sorting

The cultured osteosarcoma cell lines were trypsinized with 0.02% trypsinization-EDTA and washed with ice cold phosphate-buffered

saline (PBS) containing 1% FBS and 0.1% NaN₃. PE-conjugated mouse anti-CD133/1 monoclonal antibody (Miltenyi Biotech, Auburn, CA, USA) (1:100) or the corresponding isotype control were diluted in 3% BSA. Following 30 min of incubation with antibodies in the dark at 4°C, the cells were washed and sorted using BD FACS Aria III (BD Biosciences; San Jose, CA, USA).

Knockdown with shRNAs or siRNAs

The sorted CD133⁺ HOS cells were plated at a density of 2×10^4 cells/cm² in six-well plates and incubated in media containing polybrene (8 µg/ml; Sigma-Aldrich) overnight. Three specific *TREX1* shRNAs (shTREX1₁₋₃) and one non-specific scrambled control shRNA (shScramble) were cloned into Easy-vshRNA-mix™ lentiviral transduction vectors (Shanghai GeneChem Co, Ltd, Shanghai, China) and used to infect the cells. The media was changed 24 hours post-transfection, and the transfected cells were cultured with fresh media containing puromycin (Sigma-Aldrich) (5 µg/mL) for the selection of the corresponding clones. A pure culture was established at the time point when only transfected cells were viable. The stably-transfected cells were divided into 10 cm plates and maintained in culture.

Double-stranded siRNA against *E2F4* (siE2F4) was prepared using sense and antisense RNA oligonucleotides, as previously described (Du-Pree et al., 2004) and a non-targeting control sequence was used as a control (siCon). The cells were cultured to ~50% confluence, and transfected with siE2F4 (100 nM) using Oligofectamine (2.6 µl/ml) and Opti-MEM (10 µl/ml; Invitrogen).

Xenograft model

The animal experiments were approved by the Ethics Committee of Fujian Medical University. The cells were collected and resuspended at a ratio of 1×10^6 per 50 µl of PBS. A total of 50 µl of Matrigel (BD Biosciences) was added to each aliquot, and the cell-Matrigel suspensions were subcutaneously injected into the dorsum of 4- to 6-week-old non-obese diabetic/severe combined immunodeficiency (NOD/SCID) mice that were under anesthesia. The mice were observed for a time period of 12 weeks.

Osteosphere formation assay

Spherical colony formation assay was carried out as described by Gibbs *et al* (2005) with some modifications. The cells were plated at 2×10^3 cells per well in 6-well ultra-low attachment plates (Corning Inc., Corning, NY, USA). Fresh aliquots of epidermal growth factor (EGF) and basic fibroblast growth factor (FGF) were added every following day. On day 14, the numbers of the colonies were counted.

Migration and invasion assays

Cell invasion and migration were assayed in triplicate using 24-well Transwell inserts (8-mm pore size; Corning, CA, USA) coated with or without Matrigel (1 mg/ml; BD Biosciences) respectively. The cells (1×10^5 per well) were seeded into the upper chambers in culture media containing 0.2% FBS, and the lower chambers were filled with 500 µl of medium containing 10% FBS to induce cell migration. Following incubation for 24 h, the cells inside the chamber were removed using a cotton swab, and the migrated or invaded cells were stained with crystal violet (Lexiang Biotec, Shanghai, China) and examined using microscopy (Olympus BX61). The cells that were present in at least six randomly-selected microscopic fields ($\times 200$ magnification) were counted per well to determine the relative invasive potential.

Multilineage differentiation assay

The cells were plated at a density of 2×10^4 cells/well in 24-well plates or 2×10^5 cells/well in 6-well plates. For osteogenic differentiation, the cells were incubated in the presence of 10 mM β-glycerol phosphate and 100 µg/ml ascorbic acid for the indicated times; the induction medium was changed every 3 to 4 days. Osteogenic differentiation was assessed following 21 days of incubation. The cells were fixed with 4% formaldehyde and stained with 2% Alizarin red S (Sigma) in order to visualize the formation of calcium deposits. The cells were incubated in the presence of 100 nM dexamethasone, 250 µM iso-butyl-methyl-xanthine (IBMX), 100 µM indomethacin and 10 µg/ml insulin in order to induce adipogenic differentiation. The cultures were fixed in 4% formaldehyde and stained with Oil Red O (Sigma; 3 mg in 60% isopropanol) following 14 days of incubation in adipogenic induction medium in order

Effect of TREX1 suppression in CSC

to visualize adipogenic differentiation. The images were taken using an inverted fluorescence microscope (Nikon, Eclipse TS 100).

Cell cycle analysis

The cell cycle analysis was conducted using propidium iodide staining and flow cytometry. The cells were washed with PBS containing 0.5% BSA, and centrifuged at 2,000 rpm for 5 min. The pellets were suspended in hypotonic buffer (0.5% Triton X-100 in PBS) containing RNase and incubated for 30 min at 37°C. The cells were then incubated with 50 µg propidium iodide on ice for 30 min. Fluorescence was quantified using BD FACS Aria III. The DNA content was analyzed and the fraction of cells in the G0/G1, S and G2 phases were calculated using ModFit (Verity Software House, Topsham, ME, USA).

FACS analysis of CSC surface markers and checkpoint proteins

To measure the proportions of cells expressing specific proteins, the cells were incubated with ① CD133/1 antibody (as mentioned above); ② FITC-conjugated antibody against CD117 and APC-conjugated antibody against Stro-1 (BD Biosciences; San Jose, CA, USA); ③ PE-conjugated anti-phospho-p53 (Ser15) monoclonal antibody (BioLegend, San Diego, CA, USA); ④ anti-p21 or anti-Chk2 primary antibodies (Abcam Laboratories, Carlsbad, CA, USA), respectively with FITC/APC-conjugated goat anti-mouse IgG secondary antibody. Then the cells were fixed in paraformaldehyde 1% for 15 min, and next washed and analyzed using BD Accuri™ C6 flow cytometer (BD Biosciences; San Jose, CA, USA). At least 1×10^4 events per sample were acquired for analysis.

Cyto-immunofluorescence staining

The cells were grown on coverslips, fixed in 3.7% formaldehyde/PBS for 20 min at room temperature (RT), washed three times with PBS, blocked using 2% goat serum in 0.3% Triton X-100 in PBS and permeabilized for 5 min at RT with blocking buffer. The cells were incubated with anti-TREX1, anti-E2F4 and/or anti-OCT4 antibodies (1:100 in Triton X-100 blocking buffer) for 1 h at RT, washed three times, incubated respectively with Alexa 488- or 594-conjugated anti-rabbit/anti-mouse secondary antibodies (1:200 in Triton X-100 blocking buffer) for 45 min in the dark, rinsed three

times with blocking buffer and mounted in Vectashield containing 4,6-diamidinophenylindole (DAPI) (Vector Laboratories, Burlingame, CA, USA). The fluorescent signals were visualized using a Leica TCS-SP5 microscope (Leica Microsystems AG, Wetzlar, Germany) using a $\times 40$ magnification analysis.

The antibodies against TREX1, E2F4 were purchased from Abcam Laboratories (Carlsbad, CA, USA). The antibody against OCT-4 was purchased from Cell Signaling Technology (Danvers, MA, USA).

Immunoprecipitation and western blotting

The immunoprecipitation experiments were conducted following lysis of the cells in lysis buffer (50 mmol/L Tris at pH 7.5, 150 mmol/L NaCl, 5 µg/mL aprotinin, pepstatin, 1% Nonidet P-40, 1 mmol/L EDTA, 0.25% deoxycholate, and protease inhibitor cocktail tablet). Total cell lysates (1.0 mL) were incubated with 1 µg of anti-E2F4 overnight at 4°C and then mixed with 50 µl of the protein-G conjugated beads (Roche Molecular Biochemicals). The beads were then washed with lysis buffer, and the immunoprecipitated protein complexes were analyzed by western blotting using anti-p130, anti-E2F4, and anti-β-catenin antibodies, respectively.

Western blotting was conducted as described previously [24]. The antibodies against TREX1, E2F4, ABCB1, ABCB5, p130, c-Kit, MYB, c-MYC, CTGF, Osteocalcin, FABP-4, PPARγ, AdipoQ were purchased from Abcam Laboratories (Carlsbad, CA, USA). The antibodies against ABCG2, GSK3β, phospho-GSK3β (Ser9), β-catenin, phospho-β-catenin (Ser33/37/Thr41), TCF3, Axin2, Timp3, OCT4, ALP, Runx2 and β-actin were purchased from Cell Signaling Technology (Danvers, MA, USA).

Luciferase reporter assay

The OCT4 promoter-Luc construct was purchased from Addgene (Addgene plasmid 17221). The E2F4 promoter-Luc was constructed by inserting the E2F4 promoter (600bp), using the following primers: (forward) 5'-GC-AAAGCTTACTTGGTGGTGAGCAGTC-3', (reverse) 5'-GCAAG ATCTCAGTAGGGCAGCCTTTAG-3'. The primers were inserted into the pGL4.10 plasmid. As regards the luciferase reporter assay, the cells were grown in 24-well plates and were transfected with 0.01 µg OCT4 of luciferase reporter plasmid and 0.15 µg of β-galactosidase

Effect of TREX1 suppression in CSC

Table 1. Primer sequences

| Gene | Primer Sequences |
|--------------------------------|---|
| <i>TREX1</i> | 5'-CGTCAACGCTTCGATGACA-3' 5'-AGTCATAGCGGTCACCGTTGT-3' |
| <i>E2F4</i> | 5'-GCAGACCCACAGGTGTTTT-3' 5'-GCTCCGAGCTCATGCACTCT-3' |
| <i>ALP</i> | 5'-CACTGCGGACCATTCCCACGTCTT-3' 5'-GCGCCTGGTAGTTGTTGTGAGCATA-3' |
| <i>Osteocalcin</i> | 5'-CCCTCACACTCCTCGCCCTATT-3' 5'-AAGCCGATGTGGTCAGCCAACTCGT-3' |
| <i>Runx2</i> | 5'-CTCCCTGAAGTCTGCACCAAGTCT-3' 5'-GGGGTGGTAGAGTGGATGGACG-3' |
| <i>FABP-4</i> | 5'-AAGAAGTGGGAGTGGGCTTT-3' 5'-CTGTCTGCTGCGGTGATTT-3' |
| <i>PPARγ</i> | 5'-ACCCCTATTCCATGCTGTATG-3' 5'-AAGGAATCGCTTTCTGGGTC-3' |
| <i>AdipoQ</i> | 5'-TGGATGCTGCCATGTTCCCAT-3' 5'-CTTGTGTCTGTGTCTAGGCCTT-3' |
| <i>OCT-4</i> | 5'-AAGCGATCAAGCAGCAGACTAT-3' 5'-GGAAAGGGACCGAGGAGTACA-3' |
| <i>SOX2</i> | 5'-GCCGAACACATTGGAAGGA-3' 5'-TGCCATCAAGCAGCACTTTC-3' |
| <i>Nanog</i> | 5'-ACCTATGCCTGTGATTTGTGGG-3' 5'-AGAAGTGGGTTGTTTGCCTTTG-3' |
| <i>Klf4</i> | 5'-CCCAATTACCCATCCTTCCT-3' 5'-AGGTTTCTCACCTGTGTGGG-3' |
| <i>ABC1</i> | 5'-TGACATTTATCAAAGTAAAAGCA-3' 5'-TAGACACTTTATGCAAACATTTCAA-3' |
| <i>ABC2</i> | 5'-CCGCGACAGTTTCCAATGACCT-3' 5'-GCCGAAGAGCTGCTGAGAACTGTA-3' |
| <i>ABC5</i> | 5'-TCTGGCCCCTCAAACCTACC-3' 5'-TTTCATACCGCCACTGCCAACTC-3' |
| <i>c-KIT</i> | 5'-GTCTCCACCATCCATCCATC-3' 5'-TTTCCGACAGCACTGACTTG-3' |
| <i>MYB</i> | 5'-GCCAATTATCTCCGAATCGA-3' 5'-ACCAACGTTTCGGACCGTA-3' |
| <i>TCF4</i> | 5'-ATCCTCAGTCTGGAGCAGCAAG-3' 5'-TGAAGCAATGTGGCAACTTGGAC-3' |
| <i>c-Myc</i> | 5'-GGACAGTGTCTCTGCC-3' 5'-CGTCGCAGATGAAATAGG-3' |
| <i>Axin</i> | 5'-AGTGTGAGGTCCACGGAAAC-3' 5'-CTTCACACTGCGATGCATTT-3' |
| <i>Timp3</i> | 5'-GGCCTCAATTACCGCTACCA-3' 5'-CTGATAGCCAGGGTACCCAAAA-3' |
| <i>CTGF</i> | 5'-TTGGCAGGCTGATTTCTAGG-3' 5'-GGTGCAAACATGTAACCTTTGG-3' |
| <i>GAPDH</i> | 5'-CCCATCACCATCTCCAGGAG-3' 5'-CTTCTCCATGGTGGTGAAGACG-3' |

plasmid. Following 24 h of incubation, the transfected cells were lysed and luciferase activities were determined. Luminescence was measured using a TD-20e luminometer (Turner Design) in triplicate. The luciferase activities were normalized against the levels of β -galactosidase activity. The results represent data from three independent experiments, and error bars represent the standard deviations.

Quantitative real-time PCR

Total cellular RNA of human osteosarcoma samples, CD133⁺ OS CSCs and CD133⁻ OS non-CSCs was extracted using TRIzol reagent (Ambion, Austin, TX, USA) and treated with RNase-free DNase (DNase I, Ambion) to remove potential genomic DNA contaminants. Total RNA (1 μ g) was reverse-transcribed using the SuperScriptIII reverse transcriptase enzyme (Invitrogen) according to the manufacturer's instructions. Real-time PCR was conducted with SYBR Green PCR supermix (SangonBiotec, Shanghai, China) according to the manufacturer's instructions using an ABI Prism 7900 Sequence Detection System (Applied Biosystems). The thermal cycling conditions were as follows: 94°C for 2 min, followed by 35 cycles of 15 s at 94°C, 30 s at 60°C and 30 s at 72°C. The expression levels were normalized according to the GAPDH transcript. The primers were designed to generate a PCR product of <200 bp and the primer sequences are listed in **Table 1**.

Statistical analysis

All data were analyzed using SPSS17.0 statistical software, and presented as mean \pm standard error of measurement (SEM). The significant differences among the experimental groups were assessed using analysis of variance (ANOVA) and the appropriate post-hoc test. The differences between two experimental groups were assessed using the Student's *t*-test. A two-tailed value of $P < 0.05$ was considered significant.

Results

TREX1 expression in human osteosarcoma samples and cell lines

To investigate whether TREX1 participates in the development of osteosarcoma, the mRNA

Effect of TREX1 suppression in CSC

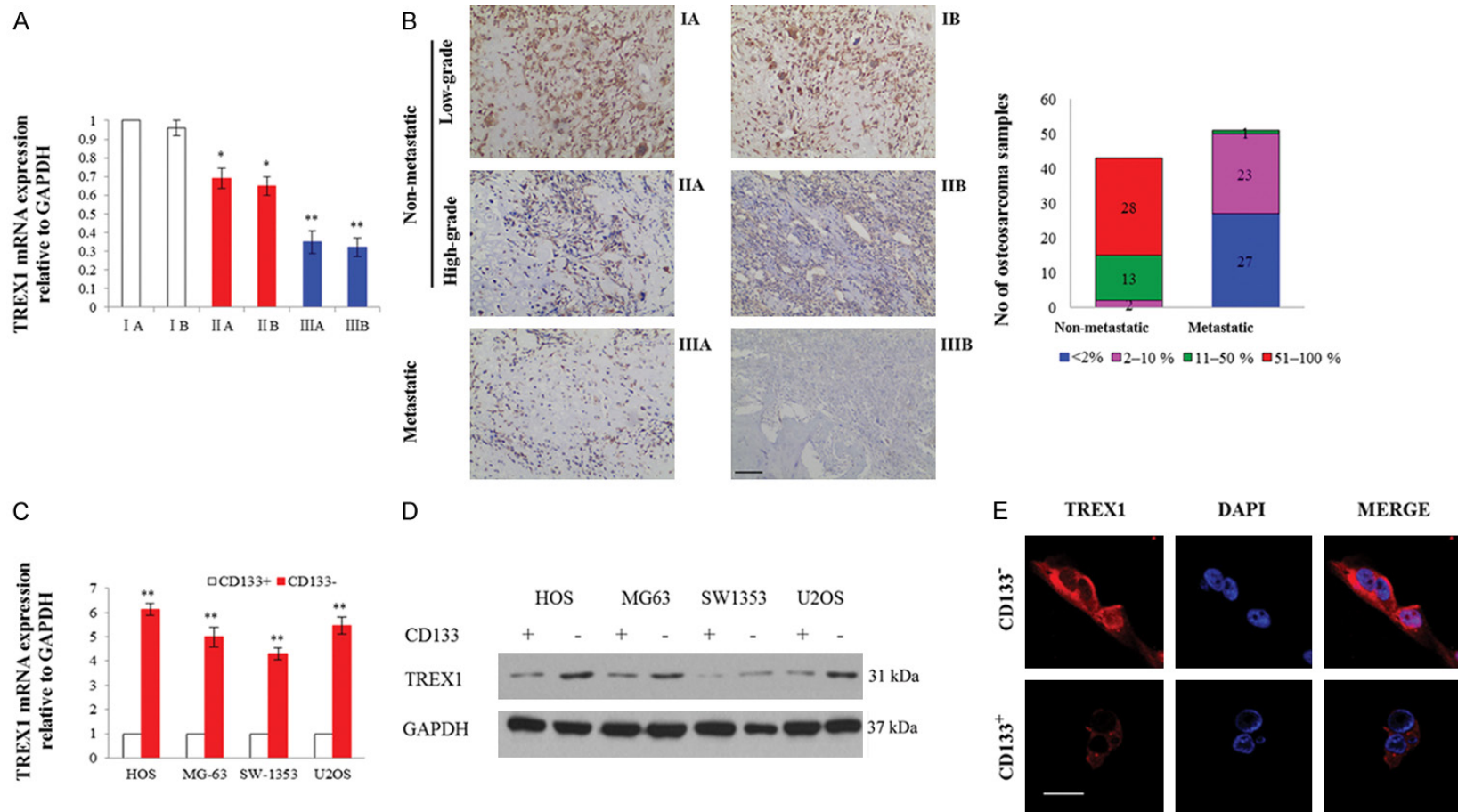


Figure 1. Expression of TREX1 in human osteosarcoma samples and cell lines. (A) Quantitative real-time PCR analysis of *TREX1* mRNA expression was carried out in human osteosarcoma samples classified by differentiation status and histologic grade. Non-metastatic: low-grade (I_A [n=5] and I_B [n=4]), high-grade (II_A [n=21] and II_B [n=13]); Metastatic: III_A [n=33] and III_B [n=18]. For every sample the PCR was carried out in triplicate. Results are expressed as means ± SEM and normalized to I_A. **P*<0.05 and ***P*<0.01 versus I_A. (B) Immunohistochemical analysis of paraffin-embedded human osteosarcoma samples with polyclonal antibody against TREX1. Representative images are shown. Scale bar indicates 100 μm. The numbers of osteosarcoma samples with varied degrees of TREX1-positive staining are shown in a proportional graph. (C, D) Quantitative real-time PCR (C) and western blotting (D) of TREX1 expression in CD133⁺ cancer stem cells (CSCs) and CD133⁻ non-CSCs derived from different osteosarcoma cell lines. For (C), results are expressed as means ± SEM and normalized to CD133⁺ CSCs. n=3, ***P*<0.01. For (D), representative images are shown. (E) Immunofluorescent staining for TREX1 (red) in CD133⁺ CSCs and CD133⁻ non-CSCs from the osteosarcoma cell line HOS; Nuclei were stained with DAPI (blue). Representative images are shown. The scale bar indicates 200 μm.

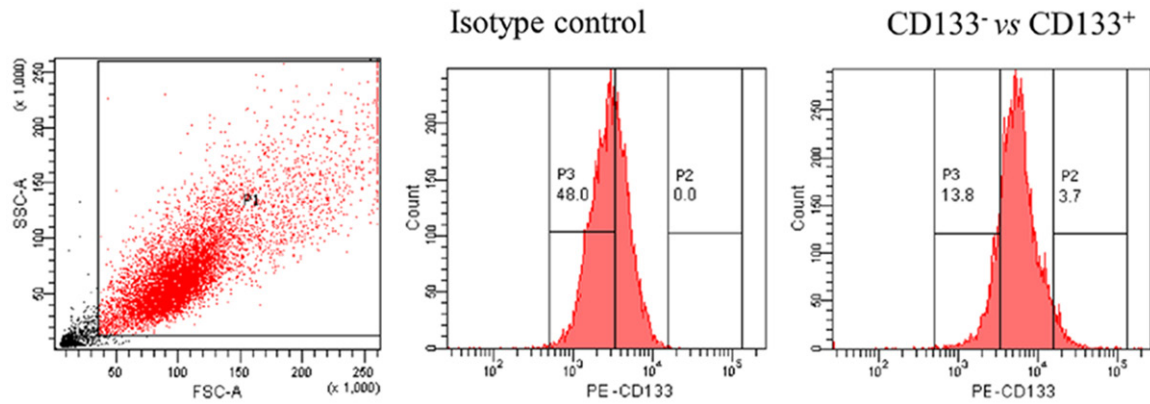


Figure 2. FACS for CD133⁻ non-CSCs and CD133⁺ CSCs from human osteosarcoma cell line HOS. Representative images of FACS for CD133⁻ HOS cells and CD133⁺ HOS cells. P2 represents CD133⁺ cells and P3 represents CD133⁻ cells.

expression of *TREX1* was examined in 94 samples of freshly-isolated tumor tissues from patients with non-metastatic low-grade (I_A [n=5] and I_B [n=4]), non-metastatic high-grade (II_A [n=21] and II_B [n=13]) or metastatic (III_A [n=33] and III_B [n=18]) osteosarcoma. The patients were 52 males and 42 females, aged 8-56 years-old (mean, 21 years-old), including 84 cases of conventional osteosarcoma (68 osteoblastic and 16 chondroblastic) and 10 cases of telangiectatic osteosarcoma. High, intermediate, and low expressions of *TREX1* mRNA were respectively observed in low-grade, high-grade, and metastatic osteosarcoma samples (**Figure 1A**). Furthermore, immunohistochemical (IHC) staining was performed to confirm the differential expression of *TREX1*. It was observed that *TREX1*-positive cells could be detected in all the tumor samples. However, the more advanced stages of the cancer were associated with the lower level of *TREX1* expression (**Figure 1B**). The data demonstrated that *TREX1* expression was negatively correlated with the degree of malignancy of osteosarcoma.

Taking into account the heterogeneity of tumor cells, we further analyzed the expression of *TREX1* respectively in CD133⁻ non-CSCs and CD133⁺ CSCs isolated from human osteosarcoma cell lines using FACS (**Figure 2**). *TREX1* mRNA and *TREX1* protein were expressed at a greater level in CD133⁻ non-CSCs compared with CD133⁺ CSCs in four types of osteosarcoma cell lines (**Figure 1C, 1D**). Confocal laser scanning further demonstrated a stronger *TREX1* peri-nuclear staining in CD133⁻ non-CSCs isolated from HOS cells (**Figure 1E**). Taken together, the data suggested that *TREX1* may

play a role in hampering the emergence of CSCs that was notably associated with the tumor severity.

TREX1 suppression endows CD133⁻ HOS cells with self-renewal ability relying on *E2F4* activation

Subsequently, the effects of *TREX1* knockdown (KD) on the features of CD133⁻ HOS cells were examined. Short-hairpin interfering RNAs (shRNAs) targeting the *TREX1* gene (sh*TREX1*₁₋₃) was used to induce a stable *TREX1*- knockdown cell line (**Figure 3**). The efficiencies of the shRNAs appeared no obvious difference. The CD133⁻ HOS cells that contained the sh*TREX1*₁ k/o plasmid were used for subsequent experiments. It was found that *TREX1* KD could promote CD133⁻ HOS cells to transform into the CD133⁺ population, while it increased the frequency of CD117⁺Stro-1⁺ cells (**Figure 4A**). In other words, *TREX1* suppression might bring about the transformation of osteosarcoma cells into CSC-like phenotypes, as indicated by the corresponding markers of tumor initiating cells [4].

Then the cell cycle of the *TREX1*-KD CD133⁻ HOS cells was analyzed. *TREX1* KD significantly increased the proportion of cells in the G2/M phase and decreased the proportion in the G0/G1 phase (**Figure 4B**). Previous studies have shown that *E2F4* is important for stable maintenance of a G2 arrest [23, 24]. *TREX1* KD was shown to significantly increase the *E2F4* mRNA and the corresponding protein expression in CD133⁻ HOS cells (**Figure 4C-E**). Further, it was found that *TREX1* KD could increase the activi-

Effect of TREX1 suppression in CSC

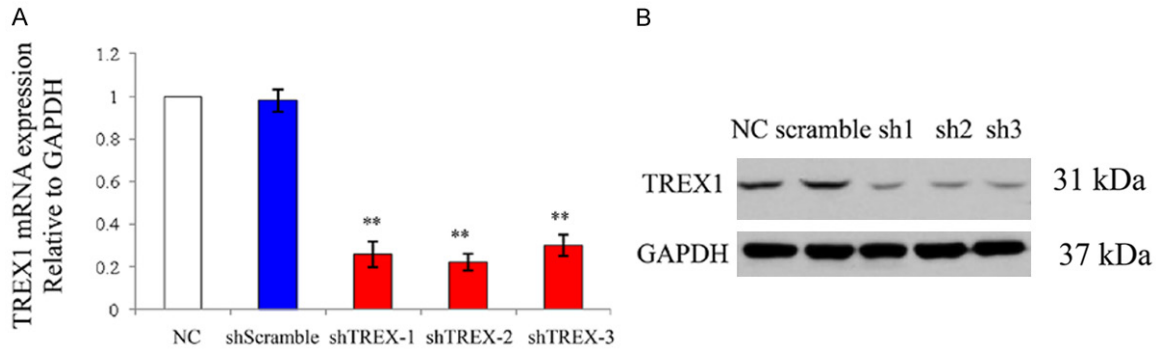


Figure 3. Confirmation of the knockdown of TREX1 in CD133⁺ HOS cells. (A) Quantitative RT-PCR and (B) western blotting analysis of TREX1 expression in CD133⁺ HOS cells transfected with shTREX1 or shScramble. For (A), results are expressed as mean \pm SEM and normalized to untreated CD133⁺ HOS cells (NC). n=3, **P<0.01 versus NC. For (B), representative images are shown.

ty of *E2F4* promoter (**Figure 5A**). The aforementioned observations and the tumorigenesis role of *E2F4* [25, 26] prompted us to investigate whether *E2F4* participates in the development of osteosarcoma at the downstream of TREX1. In contrast to the expression profile of TREX1 (**Figure 1B**), low, intermediate and high expression of *E2F4* was respectively observed in low-grade, high-grade and metastatic osteosarcoma, as determined by IHC staining (**Figure 4F**). The data suggested a link between TREX1 suppression and *E2F4* activation for the maintenance of the G2 arrest, which may contribute to the initiation and progression of osteosarcoma.

The regulatory relationship of TREX1 and *E2F4* was further examined using co-transfection with double-stranded siRNA targeting *E2F4* gene (si*E2F4*; **Figure 5B, 5C**). The co-transfection with si*E2F4* reduced the frequency of CSC-like population upon TREX1 KD (**Figure 4A**). Furthermore, the osteosphere formation assay was used to check the involvement of TREX1 and *E2F4* in affecting self-renewal ability, since the osteospheres formed in non-adherent conditions are generally considered to represent self-renewing, stem-like cells [27]. TREX1 KD significantly increased the number and size of the osteospheres formed by CD133⁺ HOS cells, when cultured in suspension in serum-free medium supplemented with EGF and FGF (**Figure 6A**). Notably, the osteospheres formed by TREX1 KD cells could be serially passaged to form secondary and tertiary osteospheres, whereas shScramble transfected cells formed only small irregular aggregates or remained as single cells that died following 3-4 days of incubation in the sphere-culture medi-

um. However, the elevated osteosphere-formation properties induced by TREX1 KD were significantly attenuated by *E2F4* KD.

Subsequently, the effect of the TREX1-*E2F4* axis on the tumorigenicity of CD133⁺ HOS cells in immuno-compromised NOD/SCID mice was investigated. First, it was observed that the tumors formed by CD133⁺ HOS cells (1×10^6 cells/mouse) were evidently larger than the tumors formed by CD133⁻ HOS cells (**Figure 7A**). However, TREX1 KD CD133⁺ HOS cells (1×10^6 cells/mouse) formed tumors within two weeks, whereas the shScramble transfected cells failed to form palpable tumors within 5 weeks. Notably, following 10 weeks of tumor implantation, the tumors formed by TREX1 KD CD133⁺ HOS cells were, approximately 6 times larger than the tumors formed by the shScramble transfected cells (**Figure 7B**). However *E2F4* KD attenuated the *in vivo* tumorigenicity-promoting effect of TREX1 KD (**Figure 7B**).

Overall, the data suggest that TREX1 KD was capable of shifting the CD133⁻ population towards the CD133⁺ population, endowing the HOS cells with self-renewal capability of CSCs, and the effect was dependent on *E2F4* activation.

TREX1 suppression and consequent *E2F4* activation in CD133⁺ HOS cells promotes metastasis and chemoresistance *in vitro*

Next the effect of the TREX1-*E2F4* axis on the metastatic potential of CD133⁺ HOS cells was investigated. TREX1 KD markedly enhanced cell migration (**Figure 6B**) and the ability of the cells to invade via Matrigel (**Figure 6C**). In con-

Effect of TREX1 suppression in CSC

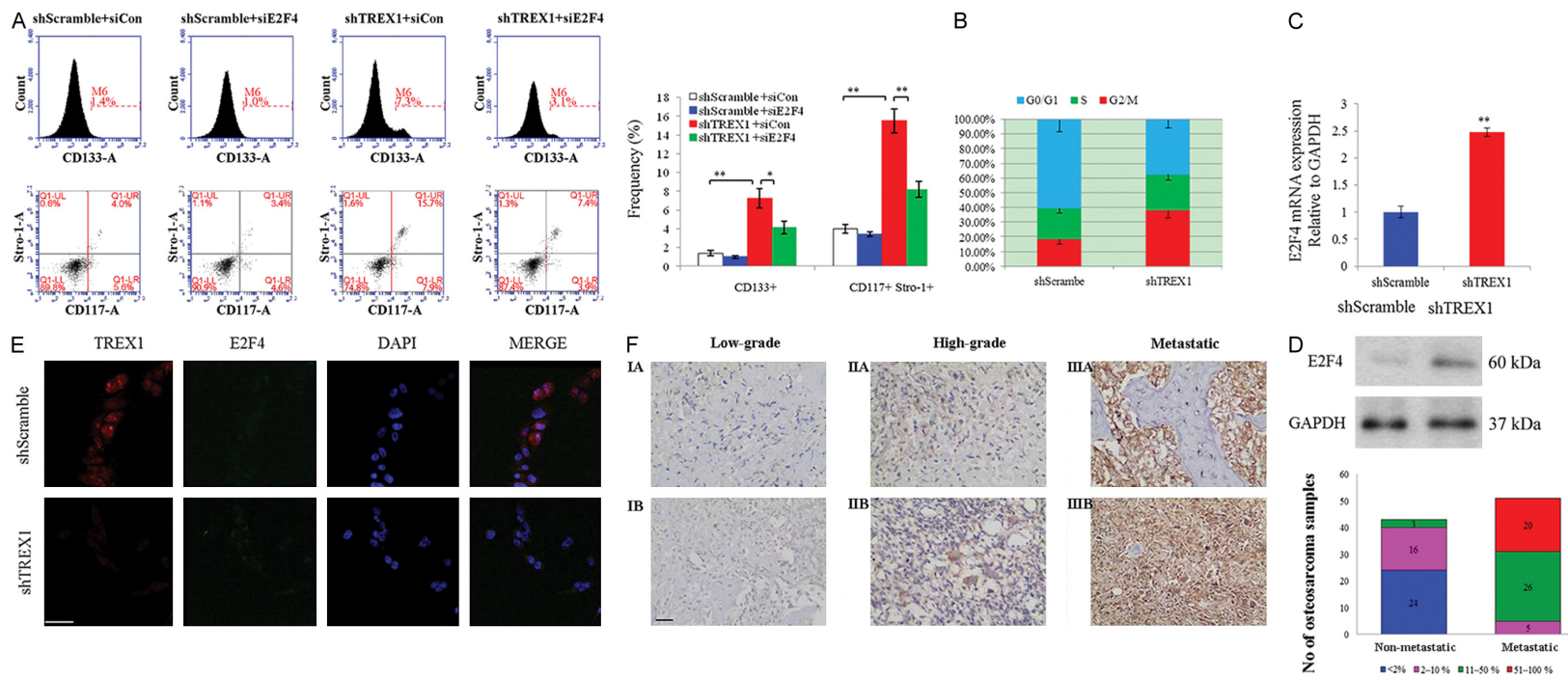


Figure 4. TREX1 knockdown (KD) promotes CSC-like phenotypes of CD133⁺ HOS cells in the dependence of E2F4. (A) The frequencies of CD133⁺ cells and CD117⁺Stro-1⁺ cells were analyzed by flow cytometry (FCM) in CD133⁺ HOS cells transfected with shTREX1 or shScramble, respectively in the presence of siE2F4 or control siRNA (siCon). Representative images are shown. Results are expressed as means \pm SEM. n=3, *P<0.05 and **P<0.01. (B) Cell cycle distribution of CD133⁺ HOS cells transfected with or shTREX1 or shScramble were analyzed using propidium iodide staining and FCM. Results are expressed as means \pm SEM. n=3. (C-E) Quantitative real-time PCR (C), western blotting (D) and representative immunofluorescent staining (E) of E2F4 expression in CD133⁺ HOS cells transfected with shTREX1 or shScramble. For (C), results are expressed as means \pm SEM and normalized to the cells transfected with shScramble. n=3, **P<0.01. For (D) & (E), representative images are shown; the scale bar in (E) indicates 200 μ m. (F) Immunohistochemical analysis of paraffin-embedded human osteosarcoma tissue samples with anti-E2F4 antibody. Representative images are shown. The scale bar indicates 100 μ m. The numbers of osteosarcoma samples with varied degrees of E2F4-positive staining are shown in a proportional graph.

Effect of TREX1 suppression in CSC

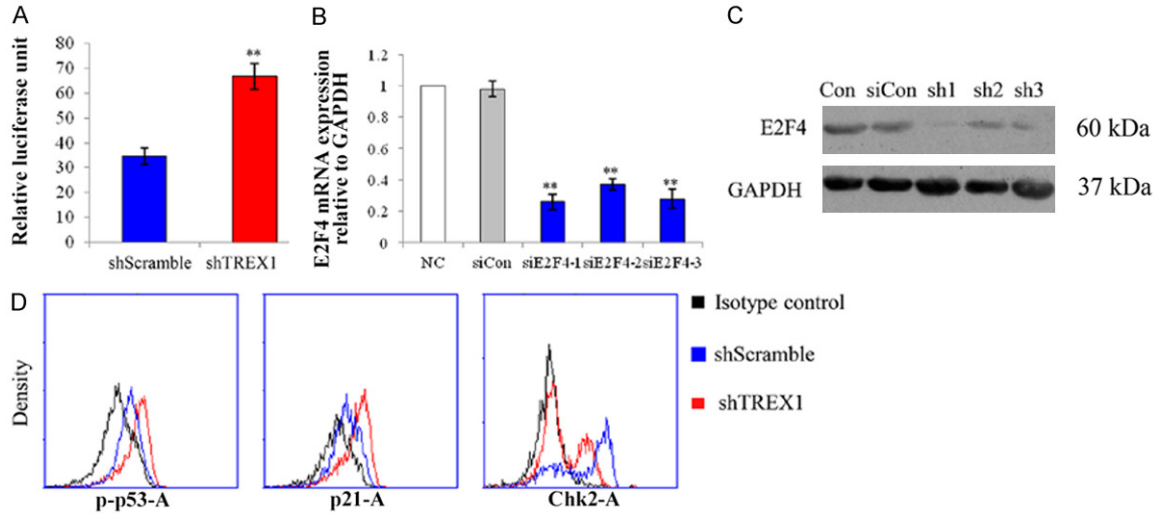


Figure 5. TREX1 KD affects checkpoint proteins involved in the regulation of G2 arrest. (A) TREX1 knockdown increased the *E2F4* promoter activity. Relative *E2F4* promoter luciferase reporter activity was measured in CD133⁺ HOS cells transfected with shTREX1 or shScramble. Results are represented as fold increase over the basal level and expressed as mean \pm SEM. $n=3$, $**P<0.01$. (B, C) Quantitative RT-PCR (B) and western blotting (C) of *E2F4* expression in CD133⁺ HOS cells transfected with siE2F4 or siCon. For (B), results are expressed as mean \pm SEM and normalized to NC. $n=3$, $**P<0.01$ versus NC. For (C), representative images are shown. (D) The frequency of cells expressing checkpoint proteins, including p-p53 (Ser15), p21 and Chk2, were analyzed by FCM in CD133⁺ HOS cells transfected with shTREX1 or shScramble.

trast to these observations, co-transfection with siE2F4 markedly reduced migration and invasion *in vitro* (Figure 6B, 6C). To examine whether the TREX1-E2F4 axis exerts an impact on the cellular response to chemotherapeutic drugs, we exposed shTREX1 or shScramble transfected cells to cisplatin or doxorubicin that are commonly used chemotherapeutic drugs for the treatment of osteosarcoma. TREX1 KD increased the chemoresistance of the CD133⁺ HOS cells (Figure 6D) that was likely associated with enhanced expression of the drug efflux pumps ABCB1, ABCG2 and ABCB5 (Figure 6E, 6F). In contrast to the chemoresistance effect caused by TREX1 KD, co-transfection with siE2F4 attenuated the resistance to chemotherapy that was exerted by TREX1 KD. Similar results were observed in doxorubicin-treated cells (data not shown). In a word, these data indicated that the metastasis and the chemoresistance of CD133⁺ HOS cells induced by TREX1 KD were dependent on E2F4 activation.

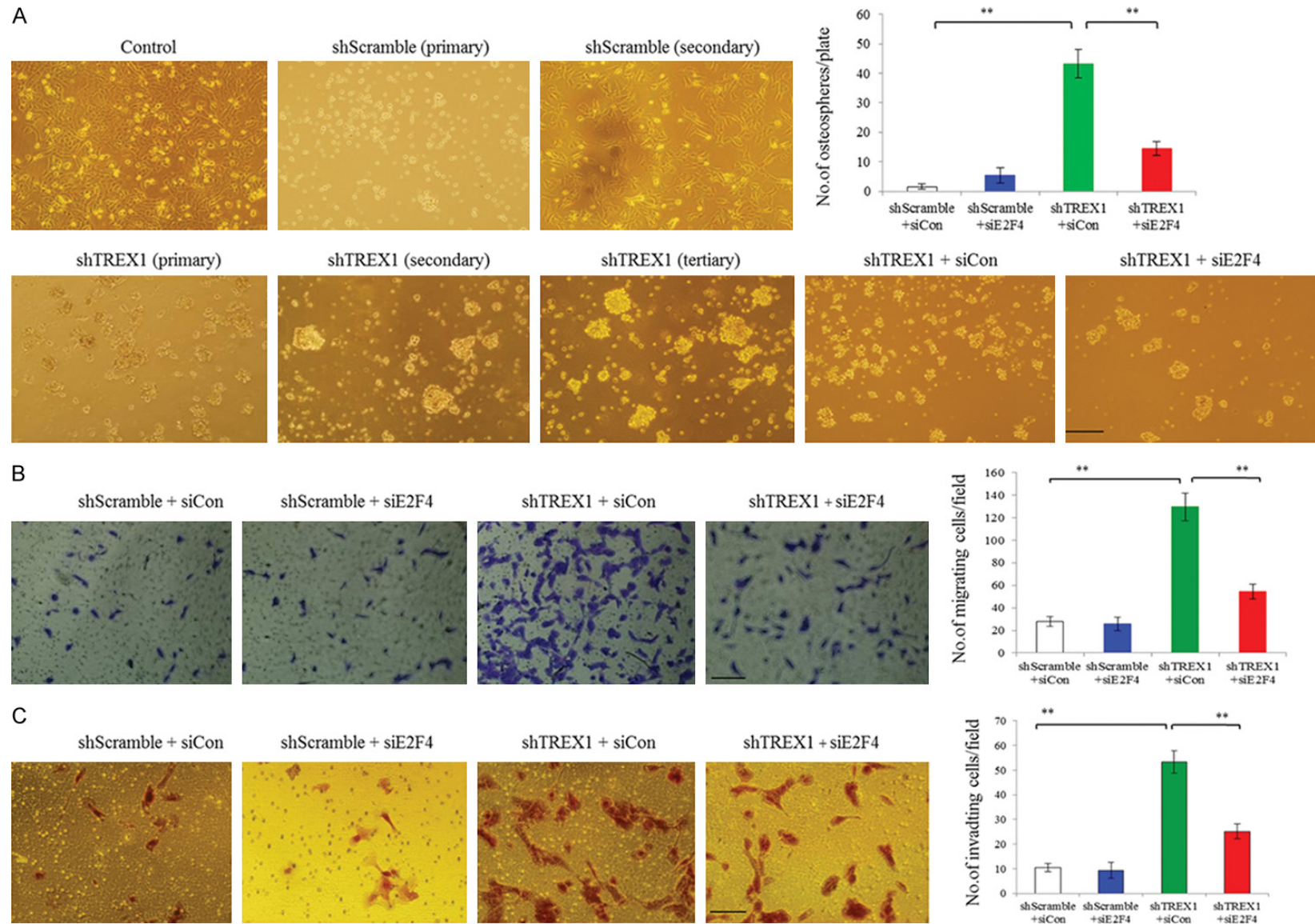
TREX1 KD in CD133⁺ HOS cells activates β -catenin signaling and elevates OCT4 through E2F4 activation

The regulatory mechanisms underlying TREX1-KD-induced CSC-like transformation of CD133⁺

HOS cells were examined, with a focus on critical molecules associated with the Wnt/ β -catenin pathway. TREX1 KD in CD133⁺ non-CSCs significantly increased p-GSK3 β and β -catenin expression (Figure 8A). Higher amounts of the p130/E2F4/ β -catenin complex were co-precipitated from TREX1 KD CD133⁺ HOS cells compared with shScramble-transfected cells; while the expression of the p130/E2F4/ β -catenin complex decreased in cells co-transfected with siE2F4 (Figure 8B). In addition, the expression (both mRNA and protein levels) of the β -catenin targets, TCF3, c-KIT, MYB and c-MYC were increased in TREX1 KD CD133⁺ HOS cells (Figure 8C, 8D); which would all be restored by siE2F4 knockdown. To sum up, the results suggested that during the transformation of CD133⁺ HOS cells towards CSCs following TREX1 KD, the elevation of β -catenin signaling in response to E2F4 activation may get involved.

Additional experiments were carried out in order to examine whether TREX1 KD could activate key stem cell transcription factors (SCTFs). A panel of key SCTFs commonly expressed in CSCs was examined. TREX1 KD significantly increased the expression of endogenous OCT-4 (Figure 9A, 9B, 9D); however, the levels of NANOG, SOX2, and KLF4 did not increase

Effect of TREX1 suppression in CSC



Effect of TREX1 suppression in CSC

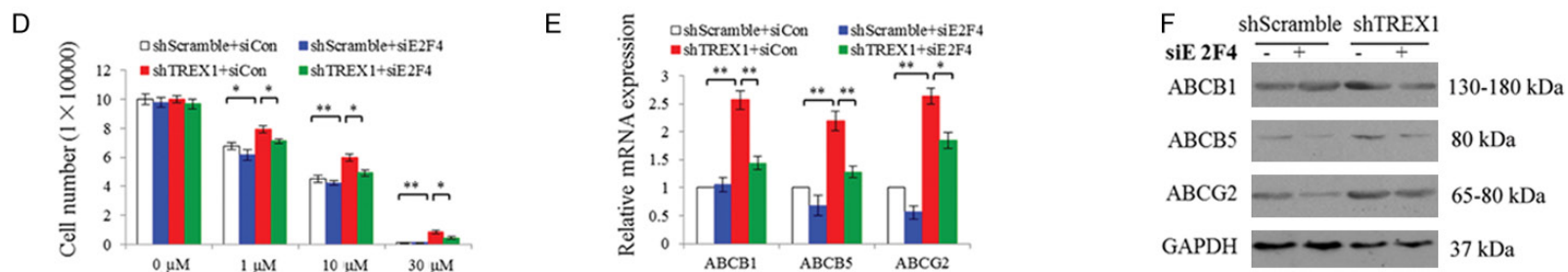


Figure 6. TREX1 KD leads to enhanced self-renewal ability, metastasis capacity, and drug resistance of CD133⁺ HOS cells *in vitro*, which are all E2F4-dependent. (A) Osteospheres formed by CD133⁺ HOS cells transfected with shTREX1 or shScramble, respectively in the presence of siE2F4 or siCon. Untreated cells were used as control. Representative phase-contrast images are shown. The scale bar indicates 200 μm. Results are expressed as means ± SEM. n=3, **P<0.01. (B) CD133⁺ HOS cells transfected with shTREX1 or shScramble, respectively in the presence of siE2F4 or siCon were subjected to the Boyden chamber cell migration assay using 10% FBS in the lower chamber as chemoattractant. The cells that migrated to the bottom of the chamber were stained with crystal violet and counted in six randomly selected fields of view per well. Representative images are shown. The scale bar indicates 100 μm. Results are expressed as means ± SEM. n=3, **P<0.01. (C) CD133⁺ HOS cells transfected with shTREX1 or shScramble, respectively in the presence of siE2F4 or siCon were seeded in the upper compartment of Matrigel-coated invasion chambers and incubated for 24 h. The cells that invaded to the bottom of the chamber were counted in six randomly-selected fields of view per well. Representative images are shown. The scale bar indicates 100 μm. Results are expressed as means ± SEM. n=3, **P<0.01. (D) CD133⁺ HOS cells transfected with shTREX1 or shScramble, respectively in the presence of siE2F4 or siCon were treated with the indicated doses of cisplatin for 24 h and cell number was counted. Results are expressed as means ± SEM. n=3, *P<0.05 and **P<0.01. (E, F) Quantitative real-time PCR (E) and western blotting (F) analysis of ABCB1, ABCG2 and ABCB5 were conducted in CD133⁺ HOS cells transfected with shTREX1 or shScramble, respectively in the presence of siE2F4 or siCon. For (E), results are expressed as means ± SEM and normalized to the cells transfected with shScramble. n=3, *P<0.05 and **P<0.01. For (F), representative images are shown.

Effect of TREX1 suppression in CSC

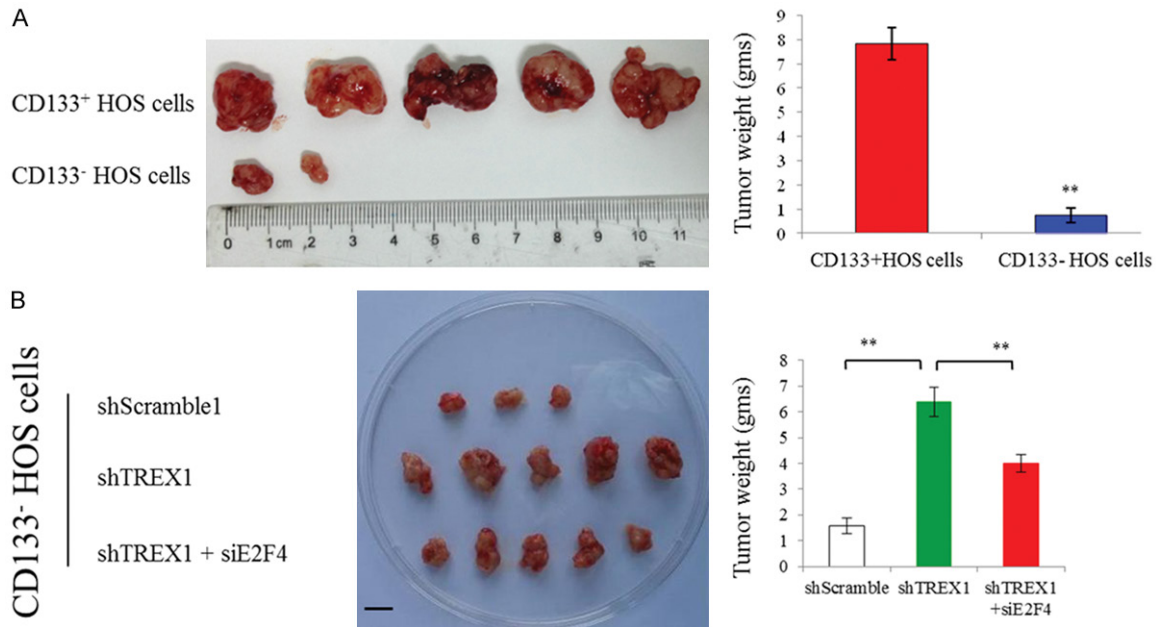


Figure 7. TREX1 KD led to enhanced tumorigenicity of CD133⁻ HOS cells *in vivo*, which is E2F4-dependent. **A.** The tumor-forming abilities of CD133⁻ and CD133⁺ HOS cells (1×10^6 cells/mouse) were assessed in NOD/SCID mice. Tumor weight was monitored bi-weekly. Representative photographs of tumors were taken ten weeks following inoculation with the tumor cells, and tumor weight was measured and expressed as means \pm SEM. $n=5$ per group, and three independent experiments for each animal, $**P<0.01$. **B.** The tumor-forming ability of CD133⁻ HOS cells transfected with shScramble, or with shTREX1 respectively in the presence/absence of siE2F4, was assessed in NOD/SCID mice. Tumor weight was monitored bi-weekly. Representative photographs of tumors were taken ten weeks following inoculation with the tumor cells, and tumor weight was measured and expressed as means \pm SEM. The scale bar indicates 1.0 cm. $n=5$ per group, and four independent experiments for each animal, $**P<0.01$.

(**Figure 9A, 9B**). TREX1 KD also significantly increased the *OCT-4* promoter activity (**Figure 9C**). Collectively, these data suggested that the CSC-like characteristics induced by TREX1 KD may be associated with increased *OCT-4* expression.

The levels of both E2F4 (**Figure 4C-E**) and *OCT-4* (**Figure 9A, 9B** and **9D**) correlated negatively with TREX1 in CD133⁻ HOS cells, and putative binding sites for E2F4 exist within 8 Kb downstream of the 3' end of the *OCT-4* gene [28, 29]. Thus consequently, we determined whether TREX1 KD-mediated *OCT-4* induction was dependent on E2F4. It showed that E2F4 KD reversed the TREX1 KD-mediated *OCT-4* induction (**Figure 9A-C**).

Taken together, the results of this work suggest a novel regulatory mechanism of TREX1 and E2F4 that affects the transformation of non-CSC tumor cells to CSC-like characteristics. TREX1 was shown to exert physical interaction with E2F4 that might lead to inhibition of the expression of the latter, as implied by immuno-

precipitation experiments. In CD133⁻ HOS cells, TREX1 suppression was demonstrated to allow the activation of β -catenin signaling in the dependence of E2F4, thus possibly leading to the upregulation of stem cell transcription factor *OCT4*; as a consequence, the non-CSC osteosarcoma cells were endowed with enhanced self-renewal ability, metastasis capacity and drug resistance *in vivo* and/or *in vitro*. The findings demonstrated that TREX1 was worth to be further studied for developing new treatments in cancer therapies targeting CSCs.

Discussion

In the present study, we provide new insights into the consequences and underlying mechanisms of TREX1 suppression in human osteosarcoma cells. TREX1 expression was found to be negatively correlated with the pathological grade and metastasis in human osteosarcoma, and it was shown to be higher in CD133⁻ non-CSCs compared to CD133⁺ CSCs in several

Effect of TREG1 suppression in CSC

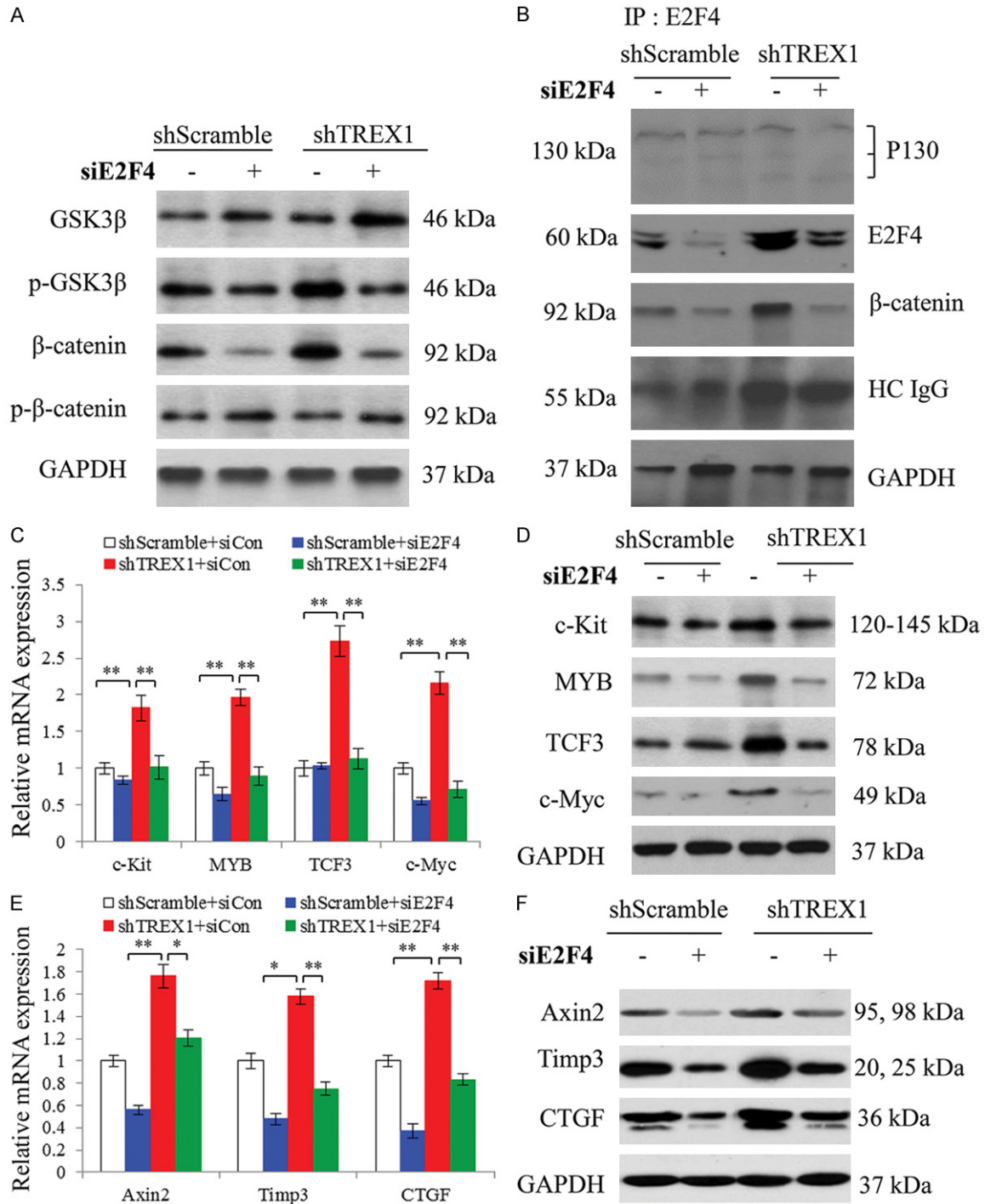


Figure 8. TREG1 KD induces the activation of WNT-β-catenin signaling in CD133⁺ HOS cells, which was E2F4-dependent. (A) Western blotting analysis of GSK3β, p-GSK3β (Ser9), β-catenin, and p-β-catenin (Ser33/37/Thr41) expression in CD133⁺ HOS cells transfected with shTREG1 or shScramble, respectively in the presence of siE2F4 or siCon. Representative images are shown. (B) Immunoprecipitation analysis of E2F4 and β-catenin in CD133⁺ HOS cells transfected with shTREG1 or shScramble, respectively in the presence of siE2F4 or siCon. E2F4 was precipitated from the cell extracts using a specific antibody; p130, E2F4 and β-catenin were detected in the precipitates by western blotting. Representative images are shown. (C, D) Quantitative real-time PCR (C) and western blotting (D) analysis of the β-catenin target genes c-KIT, c-MYC, TCF3 and MYB in CD133⁺ HOS cells transfected with shTREG1 or shScramble, respectively in the presence of siE2F4 or siCon. For (C), results are expressed as means ± SEM and normalized to the cells transfected with shScramble. n=3, **P<0.01. For (D), representative images are shown. (E, F) Quantitative real-time PCR (E) and western blotting (F) analysis of the osteoblast-specific markers Axin, TIMP3

Effect of TREX1 suppression in CSC

and CTGF in CD133⁺ HOS cells transfected with shTREX1 or shScramble, respectively, in the presence of siE2F4 or siCon. For (E), results are expressed as means \pm SEM and normalized to the cells transfected with shScramble. $n=3$, * $P<0.05$ and ** $P<0.01$. For (F), representative images are shown.

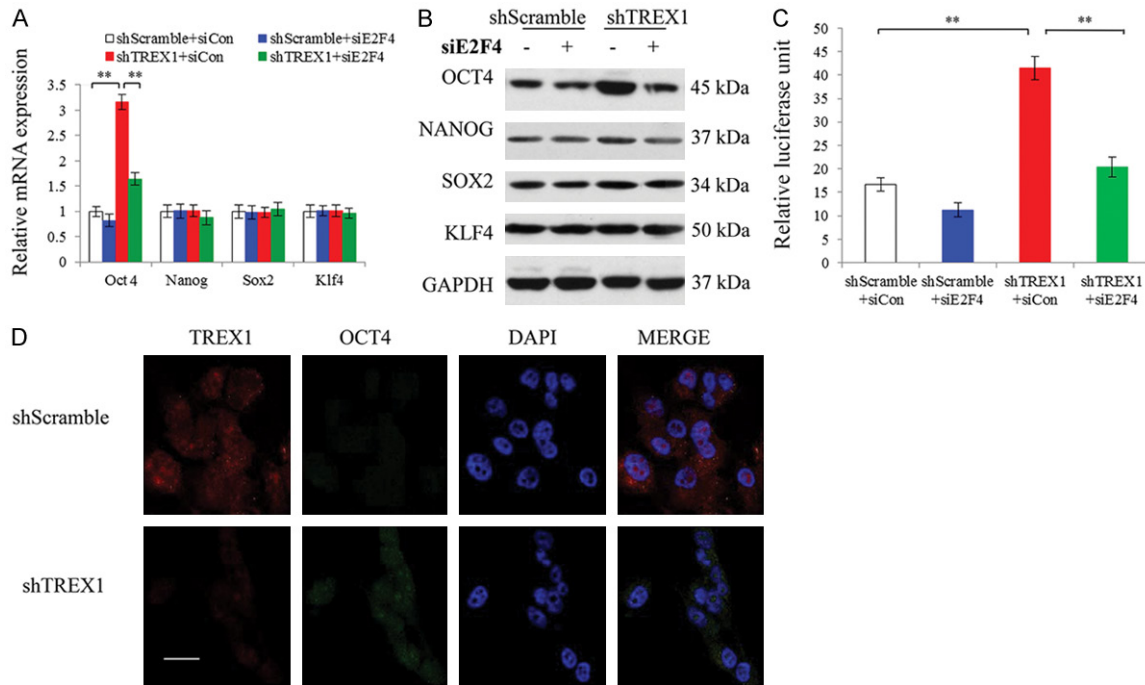


Figure 9. TREX1 KD induces OCT4 expression in CD133⁺ HOS cells, which is E2F4-dependent. (A, B) Quantitative real-time PCR (A) and Western blotting (B) analysis of OCT4, *Nanog*, *SOX2* and *KLF4* expression in CD133⁺ HOS cells transfected with shTREX1 or shScramble, respectively in the presence of siE2F4 or siCon. For (A), results were expressed as mean \pm SEM and normalized to the cells transfected with shScramble. $n=3$, ** $P<0.01$. For (B), representative images are shown. (C) Relative *OCT4* promoter luciferase reporter activity in CD133⁺ HOS cells transfected with shTREX1 or shScramble, respectively in the presence of siE2F4 or siCon. Results are presented as fold increase over the basal level and expressed as mean \pm SEM. $n=3$, ** $P<0.01$. (D) Representative immunofluorescent staining of E2F4 and OCT4 in CD133⁺ HOS cells transfected with shTREX1 or shScramble. The scale bar indicates 100 μ m.

kinds of human osteosarcoma cell lines. TREX1 knockdown (KD) endowed CD133⁺ HOS cells with enhanced self-renewal ability, metastasis capacity, and drug resistance *in vivo* and/or *in vitro*, which were all relying on E2F4. Moreover, it was found that in CD133⁺ HOS cells, TREX1 suppression would allow the activation of β -catenin signaling in the dependence of E2F4, thus possibly leading to the upregulation of stem cell transcription factor OCT4.

Several studies have provided ample evidence that non-CSCs and CSCs can inter-convert and that non-CSCs can dedifferentiate into CSCs [30, 31]. The sole overexpression of certain oncogenic molecules (e.g., OCT-4, SOX2 and Nanog) is sufficient to reprogram primary non-tumorigenic cells or bulk cancer cells into stem-like cancer cells [11, 12, 32]. To our knowledge,

this is the first study to show that TREX1 KD is plausible to impart CSC-like characteristics to human CD133⁺ non-CSCs.

The data regarding the effects of repair exonucleases on CSC emergence and the relevant mechanisms are scarce. TREX1 is considered an autonomous 3'-exonuclease that degrades DNA to prevent inappropriate immune activation. Recent genetic analysis has demonstrated that autoimmune diseases, such as Aicardi-Goutières syndrome (AGS), Systemic Lupus Erythematosus (SLE), Familial Chilblain Lupus (FCL) and Retinal Vasculopathy can be caused by mutations in TREX1, the major human 3'-5' exonuclease [17]. This is possibly attributed to chronic ATM-dependent checkpoint activation and defective transition of cell cycle, even in the absence of exogenous stress [33]. On the

Effect of TREX1 suppression in CSC

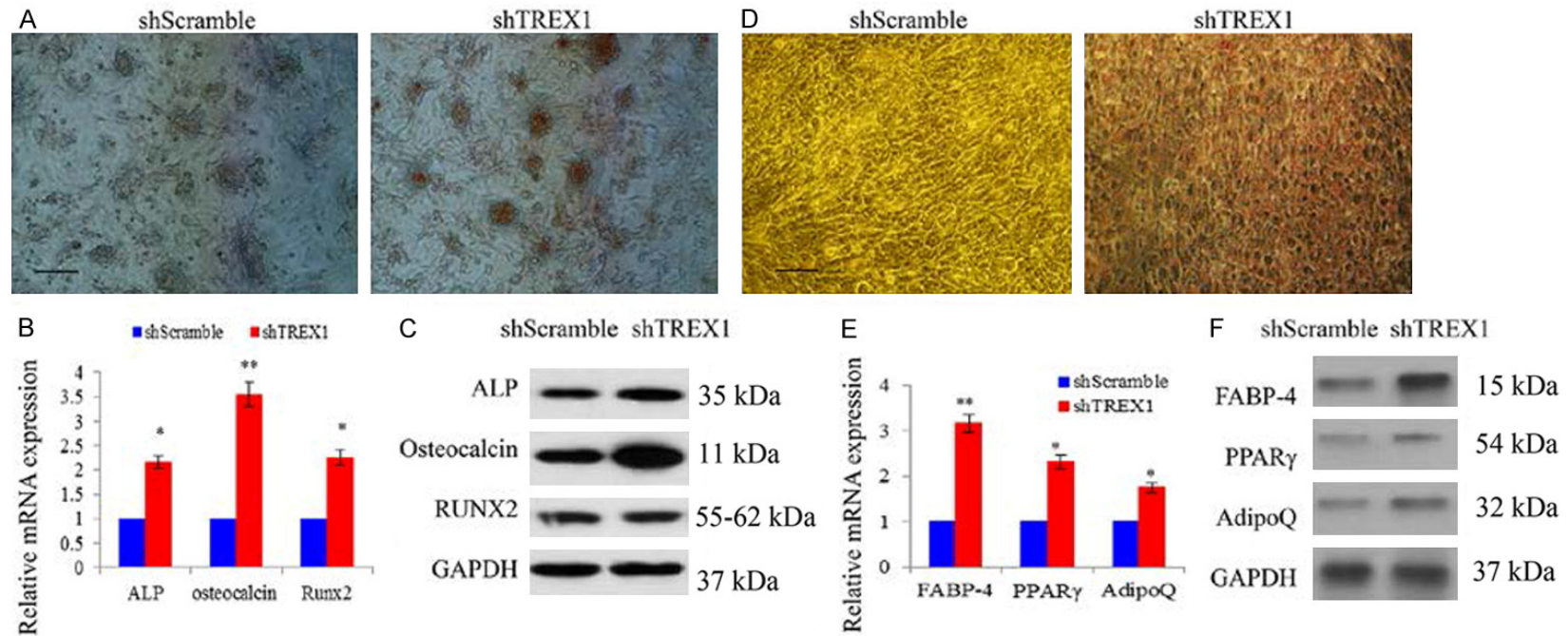


Figure 10. TREX1 KD imparts multiple differentiation potentials to CD133⁺ HOS cells. (A-C) CD133⁺ HOS cells transfected with shTREX1 or shScramble were plated in osteogenic medium and osteogenic differentiation was assessed following 21 days using alkaline phosphatase (ALP) staining. The representative plates are shown (A). The scale bar indicates 100 μ m. Quantitative real-time PCR (B) and western blotting (C) of ALP, osteocalcin and Runx2 expression were carried out. For (B), results are expressed as mean \pm SEM and normalized to the cells transfected with shScramble. n=3, * P <0.05 and ** P <0.01. For (C), representative images are shown. (D-F) CD133⁺ HOS cells transfected with shTREX1 or shScramble were plated in adipogenic medium. Adipogenic differentiation was assessed following 14 days of incubation using Oil Red O staining. Representative plates are shown (D). Scale bar indicates 100 μ m. Quantitative real-time PCR (E) and western blotting analysis (F) of FABP-4, PPAR γ and AdipoQ were carried out. For (E), results are expressed as mean \pm SEM and normalized to the cells transfected with shScramble. n=3, * P <0.05 and ** P <0.01. For (F), representative images are shown.

other hand, the inactivation of cellular division is one of the main features of cancer stem cells and it has been shown to be promoted by CDK1, a key regulator of mitosis that is involved in regulating self-renewal of stem cells, via a PDK1-PI3K/Akt signaling pathway [34]. It may be speculated that the suppression of repair exonuclease TREX1 would lead to strict restriction of the cell cycle, which might help to generate and maintain the self-renewal ability as well as other features of CSCs in tumor cells. Accordingly, the present work revealed that TREX1 suppression could increase the transcription of E2F4, which may partly account for the G2 arrest in cell cycle of CD133⁺ HOS cells with TREX1 KD. Also, the CSC-like characteristics appearing upon TREX1 KD would be reversed by E2F4 KD, which further indicated the roles of TREX1 in regulating CSC self-renewal as well as other features were E2F4 dependent. To the best of our knowledge, there are no reports on a putative role of E2F4 in CSC self-renewal, although studies have shown that abnormal expression and/or mutation of E2F4 leads to malfunction of cell cycle controls and results in carcinogenesis [25, 26]. In addition to the upregulation of E2F4, we found that TREX1 KD could also induce chronic activation of other checkpoint proteins, including increased phosphorylation of p53 and p21, and reduced Chk2 (Figure 5D) phosphorylation, which were in agreement with a previous study in *Trex1*^{-/-} mouse embryo fibroblasts (MEFs) [34].

The pro-tumorigenic role of Wnt/ β -catenin signaling, has been well described in epithelial cancers in part through the maintenance of CSCs; however, its role in tumors of mesenchymal origin remains controversial [35, 36]. Studies have demonstrated that elevated cytoplasmic and/or nuclear localization of β -catenin may be associated with metastasis in osteosarcoma [37]. Following TREX1 KD, we observed a striking increase in the activity of the Wnt pathway in CD133⁺ non-CSCs, including increased levels of active β -catenin, the endogenous β -catenin target genes TCF3, OCT-4, c-MYC and ABCB1 [10, 38]. Activation of the Wnt/ β -catenin pathway is also associated with accumulation of the p130/E2F4/ β -catenin complex [39], which in turn may activate the transcription factor TCF3 leading to the upregulation of OCT-4. The aforementioned factors are reported to

have essential roles in osteosarcoma CSC dedifferentiation and/or self-renewal [39-42].

The present work showed that the expression of OCT-4 and the activity of OCT-4 promoter were significantly increased in CD133⁺ non-CSCs with TREX1 KD, which would be reversed by co-knockdown of E2F4. Yet the expression of other SCTFs, such as Nanog, SOX-2 and KLF4 did not respond to either TREX1 KD and/or E2F4 KD. Some studies have been unable to unequivocally link the expression of the endogenous OCT4 gene/protein with tumorigenic activity, due to striking inconsistencies among the various types of assays employed [43], although the OCT4/GFP reporter was shown to be activated by the "reprogrammed" transcriptional state of the malignant cell. In contrast to this study, OCT4 has been reported to be expressed in reprogrammed sarcomas, along with other markers such as Nanog, Sox-2 and SSEA4 in studies that explored β -catenin signaling and heterogeneity of osteosarcoma cell lines in reprogramming to a pluripotent state [44, 45].

The data presented in this study are supported by previous findings where it was shown that Wnt/ β -catenin signaling is activated in CD133⁺ liver cancer stem cells, by human microRNA (miRNA), miR-1246 [46]. The latter is believed to promote cancer stemness, by activation of the Wnt/ β -catenin pathway and suppression of the expression of AXIN2 and glycogen synthase kinase 3 β (GSK3 β), two key members of the β -catenin destruction complex [46]. In addition OCT4 was identified as the direct upstream regulator of miR-1246, which cooperatively drives β -catenin activation in liver CSCs [46].

We also found that TREX1 KD could promote multiple differentiation signals, adding to the induction of CSC-like characteristics in CD133⁺ HOS cells. TREX1 KD cells exhibited a more potent ability to induce differentiation of CD133⁺ HOS cells into ALP-stained mature osteoblasts compared with scrambled shRNA (shScramble) transfected cells (Figure 10A). The results further indicated the increased expression of ALP, osteocalcin, and Runx2 (Figure 10B, 10C), whereas TREX1 KD cells exhibited increased capacity induce the adipocyte lineage, as indicated by the presence of Oil Red O-positive granules (Figure 10D) and the expression of the adipocyte-specific markers

FABP-4, PPAR γ and AdipoQ (Figure 10E, 10F). The osteoblast-specific Wnt target genes [47] such as AXIN2, TIMP3 and CTGF were increased in TREX1 KD CD133⁻ HOS cells (Figure 8E and 8F) and were downregulated during E2F4 KD. Taken together, these results indicate that TREX1 KD could impart multiple differentiation potentials to CD133⁻ HOS cells to some extent by activating E2F4. It was shown that aberrant self DNA is normally eliminated by cellular DNAses such as DNase II and TREX1, of which low amounts lead to increased levels of type I IFNs [48]; whether such a mechanism underlies our findings should be further assessed.

A few limitations of this study should be mentioned. In this study, we failed to show that cisplatin treatment *in vivo* would result in elevated amounts of CD133⁺ and OCT4-expressing tumor cells lacking TREX1, which could revert to CD133⁻ cells upon gain of TREX1 expression. Whether the loss of TREX1 would sufficiently drive stemness in CD133⁻ cells needs further confirmation. In addition, a functional assay demonstrating stemness, e.g. aldehyde dehydrogenase (ALDH) level assessment, was not performed to confirm our findings. Finally, most data were generated in HOS cells, and the observed phenotypes as well as the analyzed mechanisms should be verified in other cell lines.

In conclusion, the present study provided the first experimental evidences that TREX1 suppression with shRNA could impart CSC-like characteristics to CD133⁻ non-CSCs. Mechanistically, we found that TREX1 KD in CD133⁻ non-CSCs allowed the activation of β -catenin signaling in the dependence of E2F4, thus possibly leading to the upregulation of stem cell transcription factor OCT4. The present study suggested TREX1 was probably a negative regulator of CSC formation in tumors such as osteosarcoma and hence worth further study for developing new treatments in cancer therapies targeting CSCs.

Acknowledgements

This work was supported by grants from the National Natural Science Foundation of China (81241087, 81371331) and the Construction Project of Clinical Key Specialty of Fujian Province. We thank Dr Hengshan Zhang and Zeng Wang for their helpful suggestions.

Disclosure of conflict of interest

None.

Address correspondence to: Dr. Jianhua Lin, Department of Orthopaedics, The First Affiliated Hospital of Fujian Medical University, Fuzhou, Fujian, China. Tel: +86-13600904413; E-mail: jhlin_fyyy@126.com

References

- [1] Boman BM and Wicha MS. Cancer stem cells: a step toward the cure. *J Clin Oncol* 2008; 26: 2795-2799.
- [2] Schmohl JU and Vallera DA. CD133, selectively targeting the root of cancer. *Toxins (Basel)* 2016; 8.
- [3] Ferrandina G, Petrillo M, Bonanno G and Scambia G. Targeting CD133 antigen in cancer. *Expert Opin Ther Targets* 2009; 13: 823-837.
- [4] Adhikari AS, Agarwal N, Wood BM, Porretta C, Ruiz B, Pochampally RR and Iwakuma T. CD117 and Stro-1 identify osteosarcoma tumor-initiating cells associated with metastasis and drug resistance. *Cancer Res* 2010; 70: 4602-4612.
- [5] Dela Cruz FS. Cancer stem cells in pediatric sarcomas. *Front Oncol* 2013; 3: 168.
- [6] Calloni R, Cordero EA, Henriques JA and Bonatto D. Reviewing and updating the major molecular markers for stem cells. *Stem Cells Dev* 2013; 22: 1455-1476.
- [7] Farrugia MK, Vanderbilt DB, Salkeni MA and Ruppert JM. Kruppel-like pluripotency factors as modulators of cancer cell therapeutic responses. *Cancer Res* 2016; 76: 1677-1682.
- [8] Clarke MF, Dick JE, Dirks PB, Eaves CJ, Jamieson CH, Jones DL, Visvader J, Weissman IL and Wahl GM. Cancer stem cells—perspectives on current status and future directions: AACR workshop on cancer stem cells. *Cancer Res* 2006; 66: 9339-9344.
- [9] Mohseny AB, Szuhai K, Romeo S, Buddingh EP, Briaire-de Bruijn I, de Jong D, van Pel M, Cleton-Jansen AM, Hogendoorn PC. Osteosarcoma originates from mesenchymal stem cells in consequence of aneuploidization and genomic loss of Cdkn2. *J Pathol* 2009; 219: 294-305.
- [10] Basu-Roy U, Seo E, Ramanathapuram L, Rapp TB, Perry JA, Orkin SH, Mansukhani A and Basilico C. Sox2 maintains self renewal of tumor-initiating cells in osteosarcomas. *Oncogene* 2012; 31: 2270-2282.
- [11] Kumar SM, Liu S, Lu H, Zhang H, Zhang PJ, Gimmotty PA, Guerra M, Guo W and Xu X. Acquired cancer stem cell phenotypes through Oct4-

Effect of TREX1 suppression in CSC

- mediated dedifferentiation. *Oncogene* 2012; 31: 4898-4911.
- [12] Herreros-Villanueva M, Zhang JS, Koenig A, Abel EV, Smyrk TC, Bamlet WR, de Narvajias AA, Gomez TS, Simeone DM, Bujanda L and Billadeau DD. SOX2 promotes dedifferentiation and imparts stem cell-like features to pancreatic cancer cells. *Oncogenesis* 2013; 2: e61.
- [13] Haddox CL, Han G, Anijar L, Binitie O, Letson GD, Bui MM and Reed DR. Osteosarcoma in pediatric patients and young adults: a single institution retrospective review of presentation, therapy, and outcome. *Sarcoma* 2014; 2014: 402509.
- [14] Gillette J and Nielsen-Preiss S. Cancer stem cells: seeds of growth in osteosarcoma. *Cancer Biol Ther* 2009; 8: 553-554.
- [15] Siclari VA and Qin L. Targeting the osteosarcoma cancer stem cell. *J Orthop Surg Res* 2010; 5: 78.
- [16] Liu B, Ma W, Jha RK and Gurung K. Cancer stem cells in osteosarcoma: recent progress and perspective. *Acta Oncol* 2011; 50: 1142-1150.
- [17] Kavanagh D, Spitzer D, Kothari PH, Shaikh A, Liszewski MK, Richards A and Atkinson JP. New roles for the major human 3'-5' exonuclease TREX1 in human disease. *Cell Cycle* 2008; 7: 1718-1725.
- [18] Lehtinen DA, Harvey S, Mulcahy MJ, Hollis T and Perrino FW. The TREX1 double-stranded DNA degradation activity is defective in dominant mutations associated with autoimmune disease. *J Biol Chem* 2008; 283: 31649-31656.
- [19] Han G, Tian Y, Duan B, Sheng H, Gao H and Huang J. Association of nuclear annexin A1 with prognosis of patients with esophageal squamous cell carcinoma. *Int J Clin Exp Pathol* 2014; 7: 751-759.
- [20] Decock A, Ongenaert M, Cannoodt R, Verniers K, De Wilde B, Laureys G, Van Roy N, Berbegall AP, Bienertova-Vasku J, Bown N, Clement N, Combaret V, Haber M, Hoyoux C, Murray J, Noguera R, Pierron G, Schleiermacher G, Schulte JH, Stallings RL, Tweddle DA, Children's C, Leukaemia G, De Preter K, Speleman F and Vandesompele J. Methyl-CpG-binding domain sequencing reveals a prognostic methylation signature in neuroblastoma. *Oncotarget* 2016; 7: 1960-1972.
- [21] Dong X, Li Y, Hess KR, Abbruzzese JL and Li D. DNA mismatch repair gene polymorphisms affect survival in pancreatic cancer. *Oncologist* 2011; 16: 61-70.
- [22] Feng J, Lan R, Cai G, Lin J, Wang X, Lin J and Han D. Verification of TREX1 as a promising indicator of judging the prognosis of osteosarcoma. *J Orthop Surg Res* 2016; 11: 150.
- [23] Veselska R, Hermanova M, Loja T, Chlapek P, Zambo I, Vesely K, Zitterbart K and Sterba J. Nestin expression in osteosarcomas and derivation of nestin/CD133 positive osteosarcoma cell lines. *BMC Cancer* 2008; 8: 300.
- [24] Han D, Zhang M, Ma J, Hong J, Chen C, Zhang B, Huang L, Lv W, Yin L, Zhang A, Zhang H, Zhang Z, Vidyasagar S, Okunieff P and Zhang L. Transition pattern and mechanism of B-lymphocyte precursors in regenerated mouse bone marrow after subtotal body irradiation. *PLoS One* 2012; 7: e46560.
- [25] Schwemmle S and Pfeifer GP. Genomic structure and mutation screening of the E2F4 gene in human tumors. *Int J Cancer* 2000; 86: 672-677.
- [26] Wang D, Russell JL and Johnson DG. E2F4 and E2F1 have similar proliferative properties but different apoptotic and oncogenic properties in vivo. *Mol Cell Biol* 2000; 20: 3417-3424.
- [27] Rainusso N, Man TK, Lau CC, Hicks J, Shen JJ, Yu A, Wang LL and Rosen JM. Identification and gene expression profiling of tumor-initiating cells isolated from human osteosarcoma cell lines in an orthotopic mouse model. *Cancer Biol Ther* 2011; 12: 278-287.
- [28] Lee BK, Bhinge AA and Iyer VR. Wide-ranging functions of E2F4 in transcriptional activation and repression revealed by genome-wide analysis. *Nucleic Acids Res* 2011; 39: 3558-3573.
- [29] Boyer LA, Lee TI, Cole MF, Johnstone SE, Levine SS, Zucker JP, Guenther MG, Kumar RM, Murray HL, Jenner RG, Gifford DK, Melton DA, Jaenisch R and Young RA. Core transcriptional regulatory circuitry in human embryonic stem cells. *Cell* 2005; 122: 947-956.
- [30] Chaffer CL, Brueckmann I, Scheel C, Kaestli AJ, Wiggins PA, Rodrigues LO, Brooks M, Reinhardt F, Su Y, Polyak K, Arendt LM, Kuperwasser C, Bieri B and Weinberg RA. Normal and neoplastic nonstem cells can spontaneously convert to a stem-like state. *Proc Natl Acad Sci U S A* 2011; 108: 7950-7955.
- [31] Gupta PB, Fillmore CM, Jiang G, Shapira SD, Tao K, Kuperwasser C and Lander ES. Stochastic state transitions give rise to phenotypic equilibrium in populations of cancer cells. *Cell* 2011; 146: 633-644.
- [32] Jeter CR, Liu B, Liu X, Chen X, Liu C, Calhoun-Davis T, Repass J, Zaehres H, Shen JJ and Tang DG. NANOG promotes cancer stem cell characteristics and prostate cancer resistance to androgen deprivation. *Oncogene* 2011; 30: 3833-3845.
- [33] Wang XQ, Lo CM, Chen L, Ngan ES, Xu A and Poon RY. CDK1-PDK1-PI3K/Akt signaling pathway regulates embryonic and induced pluripotency. *Cell Death Differ* 2017; 24: 38-48.

Effect of TREX1 suppression in CSC

- [34] Yang YG, Lindahl T and Barnes DE. Trex1 exonuclease degrades ssDNA to prevent chronic checkpoint activation and autoimmune disease. *Cell* 2007; 131: 873-886.
- [35] Wang Y, Krivtsov AV, Sinha AU, North TE, Goessling W, Feng Z, Zon LI and Armstrong SA. The wnt/beta-catenin pathway is required for the development of leukemia stem cells in AML. *Science* 2010; 327: 1650-1653.
- [36] Cai Y, Mohseny AB, Karperien M, Hogendoorn PC, Zhou G and Cleton-Jansen AM. Inactive Wnt/beta-catenin pathway in conventional high-grade osteosarcoma. *J Pathol* 2010; 220: 24-33.
- [37] Iwaya K, Ogawa H, Kuroda M, Izumi M, Ishida T and Mukai K. Cytoplasmic and/or nuclear staining of beta-catenin is associated with lung metastasis. *Clin Exp Metastasis* 2003; 20: 525-529.
- [38] Ramachandran I, Ganapathy V, Gillies E, Fonseca I, Sureban SM, Houchen CW, Reis A and Queimado L. Wnt inhibitory factor 1 suppresses cancer stemness and induces cellular senescence. *Cell Death Dis* 2014; 5: e1246.
- [39] Petrov N, Zhidkova O, Serikov V, Zenin V and Popov B. Induction of wnt/beta-catenin signaling in mouse mesenchymal stem cells is associated with activation of the p130 and E2f4 and formation of the p130/Gsk3beta/beta-catenin complex. *Stem Cells Dev* 2012; 21: 589-597.
- [40] Levings PP, McGarry SV, Currie TP, Nickerson DM, McClellan S, Ghivizzani SC, Steindler DA and Gibbs CP. Expression of an exogenous human Oct-4 promoter identifies tumor-initiating cells in osteosarcoma. *Cancer Res* 2009; 69: 5648-5655.
- [41] Reya T and Clevers H. Wnt signalling in stem cells and cancer. *Nature* 2005; 434: 843-850.
- [42] Cole MF, Johnstone SE, Newman JJ, Kagey MH and Young RA. Tcf3 is an integral component of the core regulatory circuitry of embryonic stem cells. *Genes Dev* 2008; 22: 746-755.
- [43] Gibbs CP Jr, Levings PP and Ghivizzani SC. Evidence for the osteosarcoma stem cell. *Curr Orthop Pract* 2011; 22: 322-326.
- [44] Yi XJ, Zhao YH, Qiao LX, Jin CL, Tian J and Li QS. Aberrant wnt/beta-catenin signaling and elevated expression of stem cell proteins are associated with osteosarcoma side population cells of high tumorigenicity. *Mol Med Rep* 2015; 12: 5042-5048.
- [45] Choong PF, Teh HX, Teoh HK, Ong HK, Choo KB, Sugii S, Cheong SK and Kamarul T. Heterogeneity of osteosarcoma cell lines led to variable responses in reprogramming. *Int J Med Sci* 2014; 11: 1154-1160.
- [46] Chai S, Ng KY, Tong M, Lau EY, Lee TK, Chan KW, Yuan YF, Cheung TT, Cheung ST, Wang XQ, Wong N, Lo CM, Man K, Guan XY and Ma S. Octamer 4/microRNA-1246 signaling axis drives wnt/beta-catenin activation in liver cancer stem cells. *Hepatology* 2016; 64: 2062-2076.
- [47] Ambrosetti D, Holmes G, Mansukhani A and Basilico C. Fibroblast growth factor signaling uses multiple mechanisms to inhibit wnt-induced transcription in osteoblasts. *Mol Cell Biol* 2008; 28: 4759-4771.
- [48] Cheon H, Borden EC and Stark GR. Interferons and their stimulated genes in the tumor microenvironment. *Semin Oncol* 2014; 41: 156-173.